Natural Gas Conversion VIII
F.B. Noronha, M. Schmal, E.F. Sousa-Aguiar (Editors)



# Effect of cobalt on the activity of iron-based catalysts in water gas shift reaction

Amalia L.C. Pereira[a], Nilson A. dos Santos[a], Márcio L. O. Ferreira[a], Alberto Albornoz[b] and Maria do Carmo Rangel[a]

[a]*Instituto de Química, Universidade Federal da Bahia. Campus Universitário de Ondina, Federação. 40 170-280, Salvador, Bahia, Brazil*
[b]*Instituto Venezolano de Investigaciones Científicas, Apartado 21 827, Caracas 1020-A, Venezuela*

The water gas shift reaction (WGSR) is an important step in the commercial prodution of high pure hydrogen for several applications. In order to find alternative catalysts to this reaction, the effect of cobalt on the activity of iron-based catalysts was studied in this work. It was found that cobalt changed the properties of iron oxide depending on its content. In small amounts (Co/Fe(molar)= 0.05), it did not affect significantly the specific surface area but decreased the catalytic activity, a fact which can be assigned to the production of a cobalt and iron phase, less active in WGSR than magnetite. In higher amounts (Co/Fe= 1.0), cobalt led to an increase of specific surface area and to the production of cobalt ferrite and $Co_3Fe_7$ alloy, which was more active and more resistant against reduction than magnetite. This catalyst can probably work under low steam conditions, decreasing the operational costs.

## 1. Introduction

In recent years, the water gas shift reaction (WGSR) has attracted increasing interest mainly because of its application in fuel cells [1]. By WGSR, the hydrogen production from steam reforming is increased and, most importantly, the hydrogen stream is purified by the removal of carbon monoxide which often poisons most of metallic catalysts, including the platinum electrocatalyst for fuel cells [2].
The water gas shift reaction: $CO + H_2O \rightleftharpoons CO_2 + H_2$ has been widely investigated for different purposes, for instance, for ammonia synthesis and

hydrogenation reactions. Thermodynamically, the WGSR is favored by low temperatures and excess of steam, since it is exothermic ($\Delta H$= -41 kJ.mol$^{-1}$) and reversible. However, high temperatures are required for industrial applications and thus the reaction is carried out in two steps in commercial processes: a high temperature shift (HTS) in the range of 370-420 °C and a low temperature shift (LTS) at around 230 °C. The HTS step is typically performed over an iron oxide-based catalyst while the LTS stage is carried out over a copper-based one. Before its use, the HTS catalyst must be converted to magnetite ($Fe_3O_4$), which is the active phase. During this reduction, the production of metallic iron should be avoided, since it can lead to methanation and carbon monoxide disproportionation reactions [3]. In order to ensure the magnetite stability in industrial processes, large amounts of steam are added to the feed, increasing the operational costs. There is, thus, the need for developing new catalysts which can require smaller amounts of steam and can be more resistant against the magnetite reduction. With this goal in mind, this work deals with the effect of cobalt on the activity of iron-based catalysts for the HTS stage.

## 2. Experimental

Samples were prepared by mixing iron nitrate and cobalt nitrate solutions with an ammonium hydroxide solution (1% v/v) through a peristaltic pump into a beaker with water, at room temperature. Samples with cobalt to iron molar ratio of 0.05 (ICA05 sample) and 1.0 (ICA10) were obtained. The final pH was adjusted to 11 using an ammonium hydroxide solution (1%). The sol produced was stirred for additional 30 min and then centrifuged (2000 rpm, 5 min). The gel obtained was washed with water and centrifuged again. These processes were repeated several times until no nitrate ions were detected in the supernatant anymore. The gel was then dried in an oven at 120 °C, for 12 h. The solid obtained was ground and sieved in 100 mesh and then calcined at 500 ºC, for 2 h. A cobalt-free sample (IA) and an iron-free sample (CA) were also prepared to be used as references.

The catalysts were characterized by chemical analysis, specific surface area measurements, X-ray diffraction (XRD), temperature programmed reduction (TPR), X-ray photoelectron spectroscopy (XPS) and Fourier transform infrared spectroscopy (FTIR).

The iron contents were determined by X-ray dispersive energy in Shimadzu EDX-700HS model equipment. The presence of nitrate groups in the samples was verified by FTIR, using a Perkin Elmer model Spectrum One equipment, in the range of 400 to 4000 cm$^{-1}$. The XRD powder patterns of the solids were obtained in a Shimadzu model XD3A equipment, using CuK$\alpha$ ($\lambda$=0.15420 nm) radiation and nickel filter, in a 2$\theta$ range between 10-80°, in a scanning speed of 2 °/min. The specific surface area measurements were carried out by the BET method in a Micromeritics model TPD/TPR 2900 equipment, using a 30% $N_2$/He mixture. The sample was previously heated in a rate of 10 °C.min$^{-1}$ up to

160 °C, under nitrogen flow (60 mL. $min^{-1}$), for 30 min. The TPR profiles were obtained in the same equipment. The samples (0.3 g) were reduced under heating from 30 to 1000 °C, at 10 °C $min^{-1}$, using a 5% $H_2/N_2$ mixture. The XPS spectra were acquired with a VG Scientific spectrometer, Escalab model 220i-XL, with MgKα (1253 eV) anode and 400 W power, and hemispheric electron analyzer. This reference was in all cases in good agreement with the BE of the C 1s peak, at 284.6 eV.

The catalysts (0.3 g) were evaluated at 370 $^oC$ and 1 atm, in a fixed bed microreactor, with a steam to process gas (10% CO, 10% $CO_2$, 60% $H_2$ and 20% $N_2$) molar ratio of 0.6, providing there is no diffusion effect. During the experiments, the process gas was introduced into a saturator with water at 77 °C and then fed to the reactor. The products were analyzed by on line gas chromatography, using a CG-35 instrument, with Porapak Q and molecular sieve columns.

## 3. Results and Discussion

The FTIR spectra (not shown) confirmed the absence of nitrate ions in the solids. Figure 1 shows the XRD patterns of fresh and spent catalysts. Pure iron oxide (IA) displayed peaks related to hematite phase [4] while pure cobalt oxide showed the profile of the $Co_3O_4$ compound (JCPDF 87-1164). By adding small amounts of cobalt to hematite (ICA05 sample) no change in its pattern was noted. It means that cobalt was distributed in hematite lattice or formed a phase not detectable by XRD. However, when higher amounts of cobalt were added (ICA10 sample), cobalt ferrite ($CoFe_2O_4$) (JCPDF 74-2120) was produced.

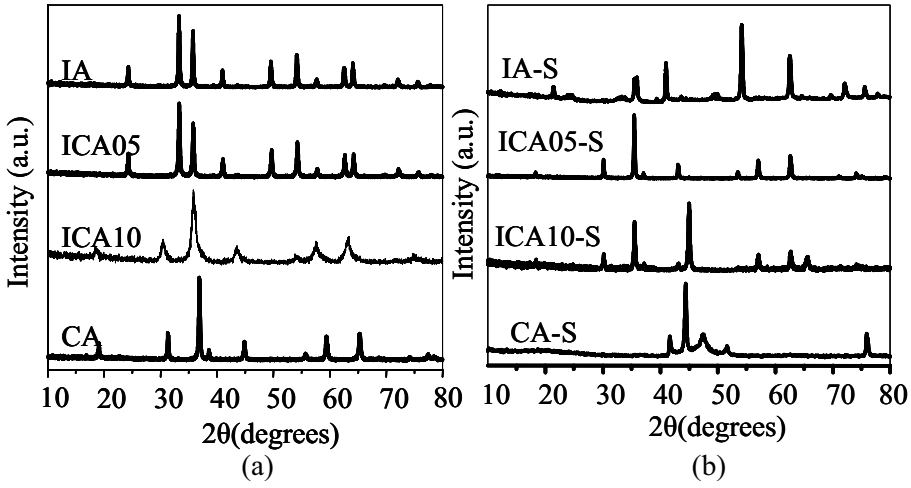


Figure 1. X-ray diffractograms of (a) fresh and of (b) spent catalysts. IA and CA samples: iron and cobalt oxide, respectively; ICA05 and ICA10 samples: with Co/Fe (molar)= 0.05 and 1.0, respectively. S represents the spent catalysts.

After WGSR, all samples showed different XRD profiles, showing that some phase transition occurred during reaction, regardless the presence of cobalt. Pure iron oxide presented a mixture of magnetite and wustite (FeO) (JCPDF 01-1121), while pure cobalt oxide showed metallic cobalt (JCPDF 75-1609 and 49-1447).On the other hand, the iron and cobalt-based samples produced different mixed phases during reaction. The sample with the smallest cobalt amount presented only the $(Co_{0,2}Fe_{0,8})Co_{0,8}Fe_{1,2}O_4$ phase (JCPDF 01-1278 and 01-1255) whereas the solid with the largest cobalt content (ICA10-S) showed cobalt ferrite ($CoFe_2O_4$) and a metallic alloy ($Co_3Fe_7$) (JCPDF 77-0426).

From the TPR curves (Figure 2a), it can be seen that cobalt changed the reduction profile depending on its amount. Iron oxide (IA) showed two peaks at 390 and 645 °C, assigned to the reduction of $Fe^{+3}$ to $Fe^{+2}$ and $Fe^{+2}$ to $Fe^0$ species, respectively [4]. The additional peak at 882 $^oC$ can be related to the reduction of the residual iron oxide in the center of the particles, which was reduced at higher temperatures. It is well-known [5, 6] that the reduction of iron oxide proceeds through a surface-controlled process; once a thin layer of iron oxide with lower oxidation state (wustite, metallic) is formed on the surface, it changes to diffusional control. Therefore, this residual nucleous does not easily access the reducing gas and thus is reduced at higher temperature where the diffusional process is faster. Cobalt oxide (CA) showed a peak at 370 °C, attributed to the reduction of $Co_3O_4$ compound; this only peak indicates that the two reduction steps ($Co_3O_4$ to CoO and CoO to Co) took place at close temperatures, as found by other authors [7]. The addition of small amounts of cobalt to iron oxide (ICA05) did not change the TPR profile, but slightly shifted the first peak (390 $^oC$) to higher temperatures (395 $^oC$), indicating that this dopant delayed the hematite reduction. A small peak appeared at low temperatures (274 °C) that can be assigned to the reduction of the $Co_3O_4$ compound [7]. It was probably present as small particles or in small amounts and then was not detectable by XRD. The high temperature peaks were shifted to even higher temperatures (660, 891 $^oC$) showing that the metallic iron production was also delayed by cobalt. On the other hand, the sample with the largest cobalt content (ICA10) presented a different profile, with three overlapped peaks (406, 534 and 648 °C), related to reduction of cobalt ferrite and a high temperature peak at 913 $^oC$, assigned to the reduction of the residual nucleous of iron oxide. Another peak, at 800 °C, can be related to the production of the $Co_3Fe_7$ alloy, detected by XRD in the spent catalysts. Therefore, this alloy was also produced in the conditions of the TPR experiments. All these peaks were shifted to higher temperatures, as compared to pure iron oxide, showing that cobalt made this solid more resistant against reduction, preserving the active phase of the catalyst.

The effect of cobalt on the specific surface area depended on its content, as shown in Table 1. It can be noted that its addition increased this property and this effect increased with its amount in solids. During WGSR, the specific surface areas decreased, indicating that the phase changes were followed by the

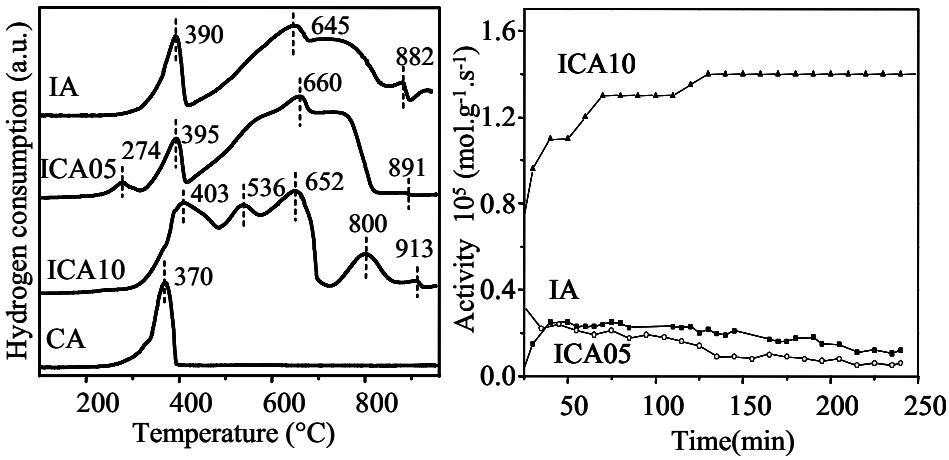


Figure 2. (a) TPR curves of the catalysts; (b) activity of the catalysts as a function of time in WGSR. IA and CA samples: iron and cobalt oxide, respectively; ICA05 and ICA10 samples: with Co/Fe (molar)= 0.05 and 1.0, respectively.

Table 1. Specific surface area of the catalysts before (Sg) and after WGSR (Sg*) and their activity (a) and the activity per area in WGSR (a/Sg*). IA and CA samples: iron and cobalt oxide, respectively; ICA05 and ICA10 samples: with Co/Fe (molar)= 0.05 and 1.0, respectively.

| Sample | Sg ($m^2g^{-1}$) | Sg* ($m^2g^{-1}$) | a.$10^5$ ($mol.g^{-1}.s^{-1}$) | a/Sg*.$10^7$ ($mol.m^{-2}.s^{-1}$) | Surface ratio Co/Fe (atom) | |
|---|---|---|---|---|---|---|
| | | | | | Fresh | Spent |
| IA | 19 | 15 | 0.12 | 0.8 | - | - |
| ICA05 | 23 | 11 | 0.06 | 0.5 | 0.094 | 0.074 |
| ICA10 | 33 | 27 | 1.40 | 5.2 | 0.078 | 2.577 |
| CA | 15 | 2 | - | - | - | - |

coalescence of particles and pores. After reaction, the sample richest in cobalt showed a specific surface area higher than pure iron oxide indicating that cobalt acted as textural promoter decreasing sinterization during the reaction.

All solids were active in WGSR, as displayed in Table 1. The addition of small amounts of cobalt (ICA05 sample) decreased the activity, as compared to pure iron oxide, but higher amounts (ICA10) did the opposite. The values of activity per area showed that this behavior can be associated to changes in active sites. In the sample with less cobalt, this fact can probably be related to a decrease in activity of the sites, due to the production of a cobalt and iron phase, less active in WGSR than magnetite. On the other hand, the increase of activity of the sample rich in cobalt can be assigned to the production of cobalt ferrite and $Co_3Fe_7$ alloy which are supposed to be the active phases. The highest activity of this sample can also be related to a textural action of the dopant, avoiding

sinterization during reaction. In fact, cobalt is able to increase the specific surface area as well as to create more active sites than pure iron oxide. From these results, it can be concluded that cobalt and iron compounds are more active than magnetite in WGSR.

Figure 2 (b) shows the activity of the catalyst as a function of time in WGSR. One can see that pure oxide, as well as the sample with small amounts of cobalt, showed stable values since the beginning of reaction. However, the catalyst with high cobalt content showed an activity which increased with time, reaching stable values after 150 min of reaction. This increase can be related to the production of the $Co_3Fe_7$ alloy, which seems to increase the activity of the catalyst.

By comparing the surface composition (Table 1) with the bulk one, it can be noted that the sample with small cobalt content (ICA05) showed a surface richer in cobalt (Co/Fe= 0.094) than the bulk (around 0.05). On the other hand, the sample richer in cobalt (ICA10) showed a surface (Co/Fe= 0.078) with less cobalt than the bulk (around 1.0). During WGSR, cobalt migrated inside the solids in different directions in each sample, depending on the cobalt amount. If high amounts of cobalt were present, the surface became richer in cobalt after reaction; if small amounts were present, an opposite behavior was observed.

## 4. Conclusions

Cobalt is an efficient dopant for iron-based catalysts for WGSR at high temperatures, when added in high amounts (Co/Fe (molar)= 1.0). Cobalt ferrite and $Co_3Fe_7$ alloy are produced in this solid, increasing the catalytic activity, as compared to pure iron oxide. In this solid, cobalt also acts as a textural promoter, increasing the specific surface area and avoiding sintering during reaction. In addition, cobalt delays the iron reduction and thus can preserve the active phase during reaction. Therefore, this catalyst can probably work under low steam conditions, decreasing the operational costs.

## References

1. G. Grubert, S. Kolf, M. Baerns, I. Vauthey, D. Farrusseng, A.C. van Veen, C. Mirodatos, E.R. Stobbe, P.D. Cobden, Appl. Catal.: A: Gen 306 (2006) 17.
2. I. Lima Júnior, J.M. Millet, M. Aouineb, M. C. Rangel, Appl Catal. A: Gen 283 (2005) 91.
3. St. G. Christoskova, M. Stoyanova, M. Georgieva, Appl. Catal. A: Gen 208 (2001) 235.
4. J. C. González, M. G. González, M. A. Laborde and N. Moreno, Appl. Catal., 20 (1986) 3.
5. T. Wiltowski, K. Piotrowski, H. Lorethova, L. Stonawski, K. Mondal, S.B. Lalvani, Chem. Eng. Proc. 44 (2005) 775.
6. K.Piotrowski, K. Mondal, H. Lorethova, L. Stonawski, T. Szymański, T. Wiltowski, Int. J. Hydrogen Energy 30 (2005) 1543.
7. W.J. Wang, Y.W. Chen, Appl. Catal. 77 (1991) 223.